

Sensor and Simulation Notes

Note 534

October 2008

Analytical Calculations of a Lens for Launching a Spherical TEM Wave

Serhat Altunc, Carl E. Baum, Christos G. Christodoulou, Edl Schamiloglu

University of New Mexico
Department of Electrical and Computer Engineering
Albuquerque New Mexico 87131

Abstract

An electromagnetic lens is designed to obtain better launching for a prolate-spheroidal IRA. Within the lens we have a spherical TEM wave centered on the switch center. However, outside the lens we have an approximate spherical TEM wave which is centered at the first focal point of the prolate-spheroidal IRA.

1. Introduction

Designing the feed point is one of the most important concerns that one should consider to obtain a fast-rising (100 ps) spherical TEM wave. Diverging a spherical TEM wave to another diverging spherical TEM wave is the key point of this design. A uniform dielectric lens can be used to ensure the launching of an approximate spherical TEM wave onto the TEM feed arms of our prolate-spheroidal IRA. We design a lens such that within the lens we have a spherical TEM wave centered on the switch center. However, outside the lens we have an approximate spherical TEM wave which is centered at the first focal point of the prolate-spheroidal IRA. High-pressure hydrogen can be used as an insulating medium containing the switch. The risetime of the pulser is about 100 ps. The dimensions of the lens geometry can be calculated as in [1,2,3]. However, we should manipulate the equations and change the constraints that are suitable for our prolate-spheroidal IRA design. The larger lens gives us less dielectric breakdown. However, we have to deal with loss and dispersion as a price for larger dimensions. Determining the dimensions of the lens is also a numerical and experimental problem. One should consider the dielectric breakdown for the lens dimension determination. More detailed numerical simulations should be done to determine the optimum geometry. Figure 1 shows the prolate-spheroidal and launching lens geometry.

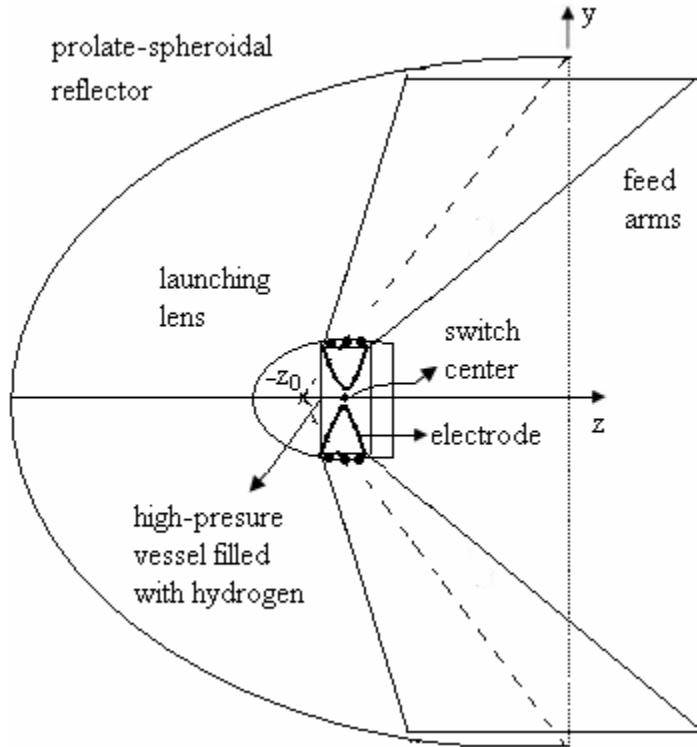


Figure 1. 60° Four-Arm Prolate-spheroidal IRA and launching lens geometry.

2. Lens Design

Diverging a spherical TEM wave to another diverging spherical TEM wave is discussed in [1]. Lens for launching spherical TEM wave is depicted in Figure 2.

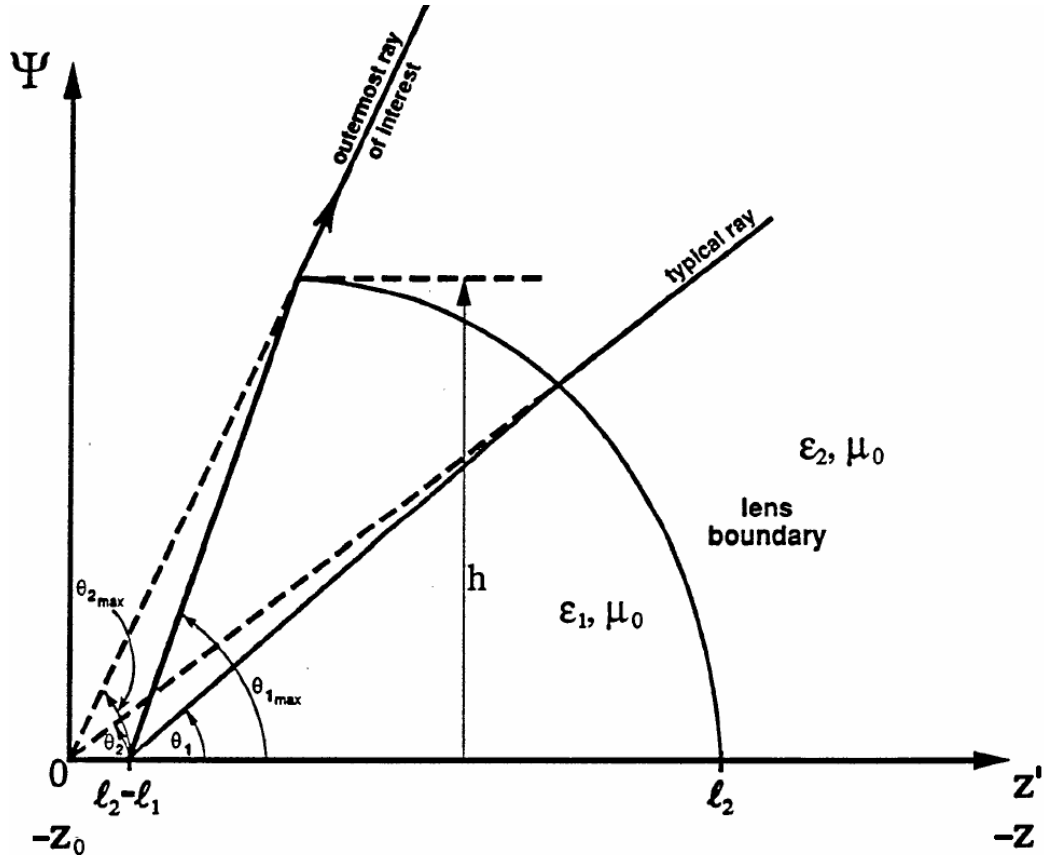


Figure 2. Lens For Launching Spherical Wave[1].

ℓ_1 and ℓ_2 are the distances from the launch point and focal point to the lens boundary on the z -axis, respectively. h is the height of the lens. We define a new coordinate called the z' - coordinate, where 0 corresponds $-z_0$ in this new coordinate (as in [1]). θ_{1max} is the angle between the z' -axis (or $-z$ -axis) and the center of the feed arm. θ_{2max} is the angle between the z' -axis(or $-z$ -axis) and the switch center. The normalized ℓ_1 and ℓ_2 parameters can be defined from (5.7) in [1] as

$$\begin{aligned}\frac{\ell_1}{h} &= \frac{\sin(\theta_{1max} - \theta_{2max}) + \varepsilon_r^{1/2} \sin(\theta_{2max}) - \sin(\theta_{1max})}{(\varepsilon_r - 1)^{1/2} \sin(\theta_{1max}) \sin(\theta_{2max})} \\ \frac{\ell_2}{h} &= \frac{\varepsilon_r^{1/2} [\sin(\theta_{1max} - \theta_{2max}) + \sin(\theta_{2max})] - \sin(\theta_{1max})}{(\varepsilon_r - 1)^{1/2} \sin(\theta_{1max}) \sin(\theta_{2max})}\end{aligned}\quad (2.1)$$

In [1] $\theta_{2max} < \theta_{1max} \leq 90^\circ$ as seen in figure 2. However, in our case $90^\circ = \theta_{1max} < \theta_{2max}$ as shown in Figure 3. One can calculate θ_{2max} from figure 3 as

$$\theta_{2max} = \pi - \arctan(b/z_0), \quad 0 \leq \theta_2 \leq \theta_{2max} \quad (2.2)$$

This represents the range of interest of incoming-wave angles from the prolate-spheroidal IRA which has the dimensions as [4]

$$b = \Psi_0 = .5m, \quad a = .625m, \quad z_0 = .375m. \quad (2.3)$$

Where a and b are the radii and z_0 is the focal distance of the prolate-spheroidal IRA. From (2.2) and (2.3), one can easily calculate the θ_{2max} , and it is 127° .

The waves have to look like spherical wave emanating from virtual focus. Therefore,

- We need external rays to come from a surface surrounding the virtual focus.
- Hence the z intersection point is to right of the focus.

The equal-time condition for a diverging spherical wave in a medium with permittivity $\varepsilon_r \varepsilon_0$ going into another diverging spherical wave in a second medium with ε_0 can be written as

$$\sqrt{\varepsilon_r} r_{1b} + r_2 - r_{2b} = \sqrt{\varepsilon_r} \ell_1 + r_2 - \ell_2 \quad (2.4)$$

r_2 is the radius of the spherical TEM wave centered at the focal point, r_{1b} , r_{2b} are the distances from launch and focal point to the lens boundary, respectively. z_b and Ψ_b are the z and Ψ values that correspond to this boundary point.

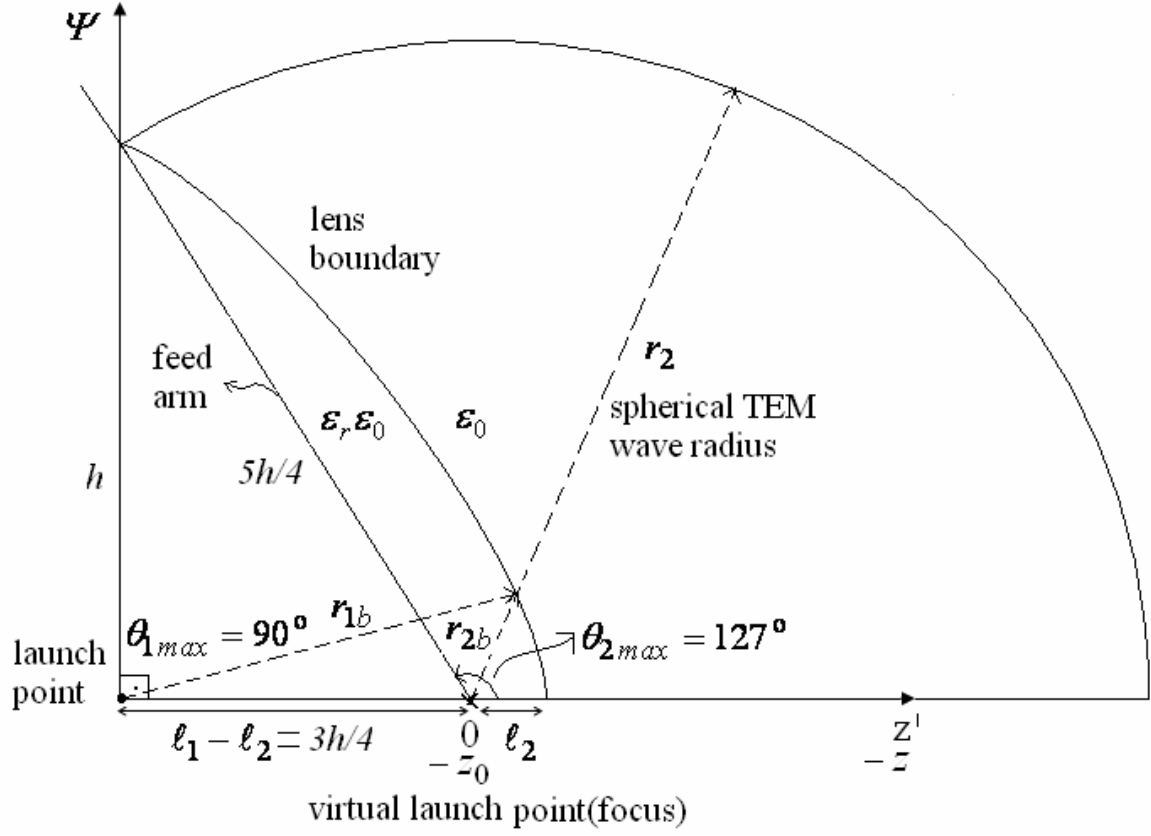


Figure 3. Launching Lens Geometry

r_{1b} and r_{2b} can be written as

$$\begin{aligned} r_{1b} &= \left[(\ell_1 - \ell_{21} + z_b)^2 + \Psi_b^2 \right]^{1/2}, \\ r_{2b} &= [z_b^2 + \Psi_b^2]^{1/2}. \end{aligned} \quad (2.5)$$

Substituting (2.5) in (2.4) gives

$$\sqrt{\varepsilon_r} \left[\left[(\ell_1 - \ell_{21} + z_b)^2 + \Psi_b^2 \right]^{1/2} - \ell_1 \right] = [z_b^2 + \Psi_b^2]^{1/2} - \ell_2. \quad (2.6)$$

The equal time condition equation for our case gives the same equation as in (5.1) of [1].

To find θ_2 as a function of θ_1 a quadratic equation in either $\cos(\theta_2)$ or $\sin(\theta_2)$ can be solved from (5.8-5.10) in [1] as

$$\begin{aligned}
\cos(\theta_2) &= \frac{AB\sin^2(\theta_l) \pm \left|B\cos(\theta_l) - A\varepsilon_r\right|^{1/2} \sqrt{\left[B^2 - 2AB\varepsilon_r\cos(\theta_l) + A\varepsilon_r\right] - A^2\sin^2(\theta_l)}}{B^{1/2} - 2AB\varepsilon_r\cos(\theta_l) + A\varepsilon_r} \\
\sin(\theta_2) &= \frac{A(A\varepsilon_r - B\cos(\theta_l)) \pm |B|\sin(\theta_l) \sqrt{\left[B^2 - 2AB\varepsilon_r\cos(\theta_l) + A\varepsilon_r\right] - A^2\sin^2(\theta_l)}}{B^{1/2} - 2AB\varepsilon_r\cos(\theta_l) + A\varepsilon_r} \\
A &= (\ell_2/\ell_1) - 1, \quad B = (\ell_2/\ell_1) - \varepsilon_r
\end{aligned} \tag{2.7}$$

However in our case, we have manipulated the equations in [1] for our special case of $\theta_{1max}=90^\circ$ and $\theta_{2max}=127^\circ$. Equation (2.4) has both \pm roots, while in [1] just + roots are considered. We have to consider both roots and take the roots that physically fit our design.

A lens boundary curve can be defined by the coordinates of z' and Ψ as a function of θ_1 and θ_2 from (2.7) as

$$\begin{aligned}
\frac{z'}{h} &= \frac{(\ell_2 - \ell_1)/h \tan(\theta_1)}{\tan(\theta_1) - \tan(\theta_2)} \\
\frac{\Psi}{h} &= \frac{z}{h} \tan(\theta_2) = \frac{(\ell_2 - \ell_1)/h \tan(\theta_1) \tan(\theta_2)}{\tan(\theta_1) - \tan(\theta_2)}
\end{aligned} \tag{2.8}$$

2.1 Calculating the minimum $\sqrt{\varepsilon_r}$

The wave should propagate from the launch point to lens boundary in the same time horizontally and vertically. One can write the equal-time condition for waves that propagate vertically and horizontally as

$$\sqrt{\varepsilon_r}h = \sqrt{\varepsilon_r}3h/4 + \sqrt{\varepsilon_r}\ell_2 + 5h/4 - \ell_2 \tag{2.9}$$

ℓ_2 can be written in terms of $\sqrt{\varepsilon_r}$ from (2.9) as

$$\ell_2 = \frac{h[\sqrt{\varepsilon_r} - 5]}{4[\sqrt{\varepsilon_r} - 1]} \tag{2.10}$$

$\ell_2 \geq 0$ therefore from (2.10)

$$\varepsilon_r \geq 25. \tag{2.11}$$

2.2 Calculating Angles Related to the Lens Boundary

One can see write the Snell's Law for the given lens-boundary angles as

$$\sqrt{\varepsilon_r} \sin(\theta_i) = \sin(\theta_t) \quad (2.12)$$

The angles related to the lens boundary are presented in figure 4. As one can see in figure 4

$$\theta_t - \theta_i = a \tan(3/4) = 37^\circ \quad (2.13)$$

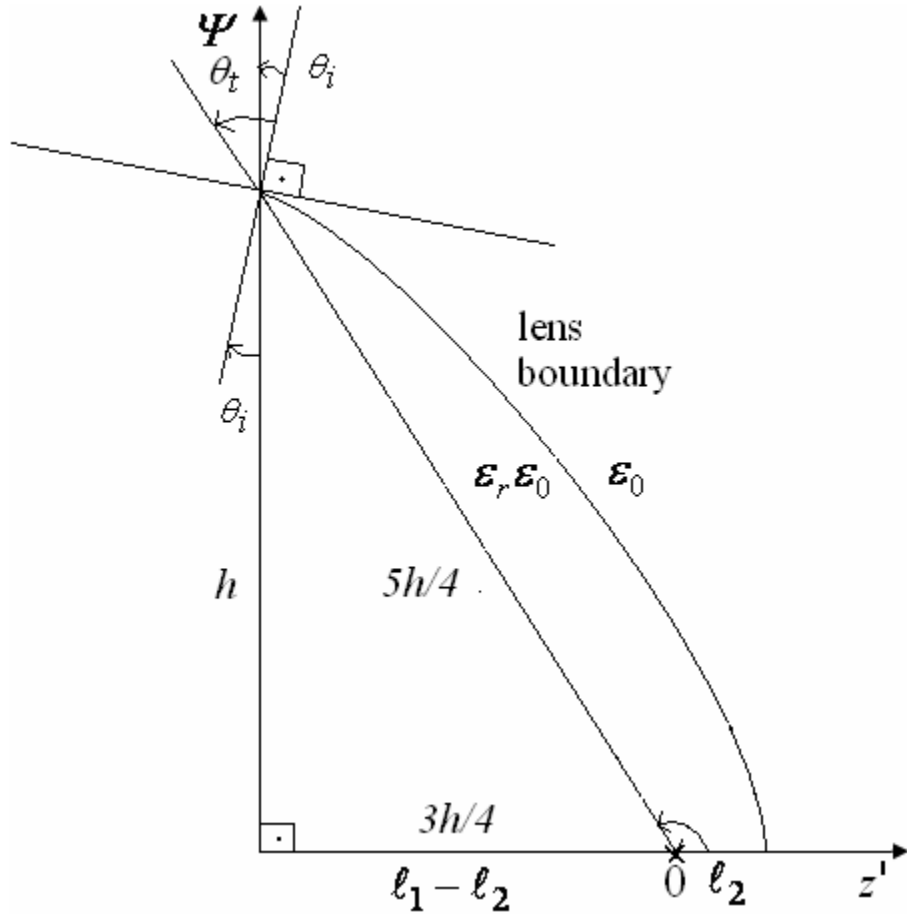


Figure 4. Angles at the Lens Boundary

From (2.12) and (2.13) one can calculate θ_i in terms of ε_r as

$$\theta_i = a \tan \left(\frac{\cos(a \tan(3/4))}{\sqrt{\varepsilon_r} - \sin(a \tan(3/4))} \right) = a \tan \left(\frac{0.6}{\sqrt{\varepsilon_r} - 0.8} \right). \quad (2.14)$$

Table 1 presents the θ_i , ℓ_1/h and ℓ_2/h values for different ε_r values.

Table 1. θ_i , ℓ_1/h and ℓ_2/h values for different ε_r

ε_r	25	36	49
θ_i (Degrees)	8.1	6.6	5.5
ℓ_1/h	0	0.05	0.08
ℓ_2/h	0.75	0.8	0.83

One can see from table 1 that if we increase ε_r value, we obtain smaller θ_i and bigger ℓ_1/h and ℓ_2/h values. Furthermore, we note that the positive θ_i values indicate that the lens boundary has $\Psi \leq h$ for physical lens angles.

3. Launching Lens Design: From Lens to Air

Let us consider the simplest case for which the wave propagates from lens to air.

There are two ways to find the curve of the launching lens boundary. One can solve (2.6) numerically. We can also change $0 \leq \theta_1 \leq 90^\circ$ and calculate θ_2 values from (2.7), from θ_1 and θ_2 values a lens boundary curve can be defined by the coordinates of z'/h and Ψ/h as functions of θ_1 and θ_2 . We call the first technique numerical and second one analytical. Figures 5,6 show the numerical and analytical solutions for $\varepsilon_r = 25, 36$ and tables 2,3 present the θ_{1max} , θ_{2max} , z'/h and Ψ/h values for $\varepsilon_r = 25, 36$, respectively. Finally, figure 7 shows the analytical solution for $\varepsilon_r = 49$ case and table 4 presents the θ_{1max} , θ_{2max} , z'/h and Ψ/h values for $\varepsilon_r = 49$.

As discussed before, we should be careful to pick the right roots, otherwise we'll have an unphysical solution. For analytical solution, we consider both \pm roots. However, for $\varepsilon_r = 25$ roots give the physical solution. For $\varepsilon_r = 36$, we pick the $-$ roots for the first five roots and $+$ roots for the others. When $\varepsilon_r = 49$, we pick the $-$ roots for the first six roots and $+$ roots for the others. One can see from figure 5,6 the analytical and numerical solution curves fit as expected.

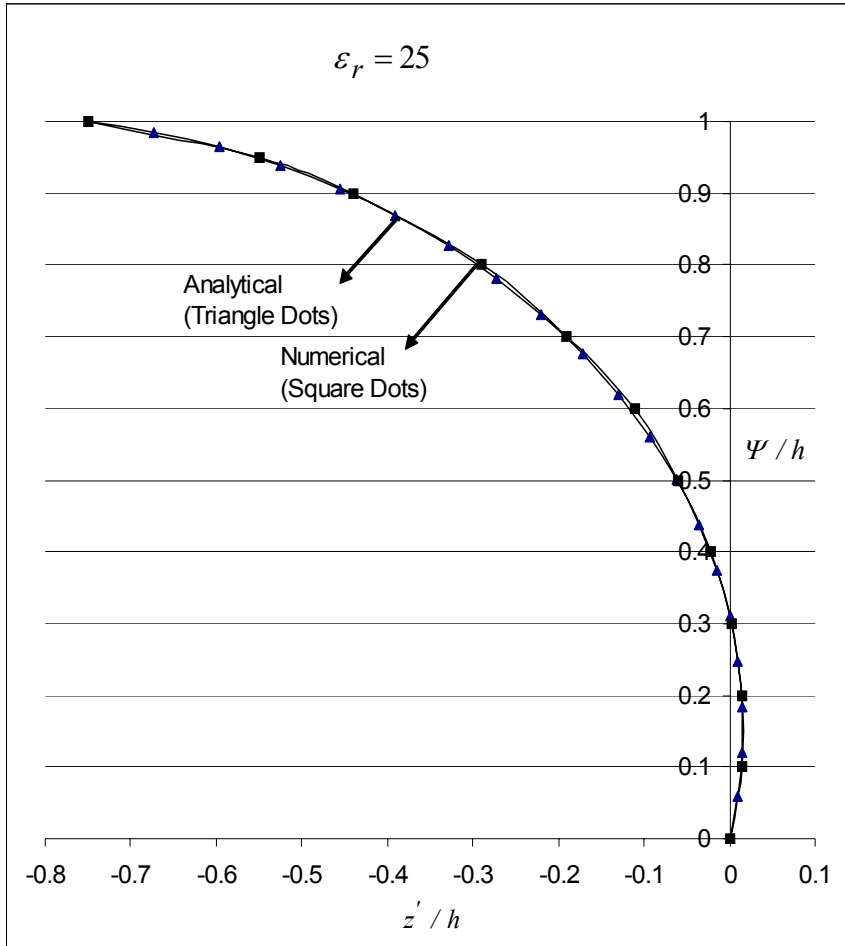


Figure 5. Lens Boundary Curve Analytical and Numerical Solution for $\varepsilon_r = 25$

Table 2. θ_{1max} , θ_{2max} , z' / h and Ψ / h Values for $\varepsilon_r = 25$

A n a l y t i c a l			N u m e r i c a l		
θ_1 °	θ_2 °	z' / h	Ψ / h	z' / h	Ψ / h
0	0	0	0	0	0
4.5	80.723	0.010	0.060	0.014	0.1
9	82.999	0.015	0.121	0.015	0.2
13.5	85.294	0.015	0.184	0.003	0.3
18	87.607	0.010	0.247	-0.022	0.4
22.5	89.938	0.000	0.311	-0.06	0.5
27	92.286	-0.015	0.375	-0.11	0.6
31.5	94.652	-0.036	0.438	-0.19	0.7
36	97.035	-0.062	0.500	-0.29	0.8
40.5	99.435	-0.093	0.561	-0.44	0.9
45	101.852	-0.130	0.620	-0.55	0.95
49.5	104.285	-0.172	0.676	-0.75	1
54	106.735	-0.220	0.730		
58.5	109.200	-0.272	0.780		
63	111.681	-0.329	0.827		
67.5	114.178	-0.390	0.869		
72	116.688	-0.456	0.906		
76.5	119.214	-0.525	0.938		
81	121.752	-0.597	0.965		
85.5	124.305	-0.672	0.986		
90	126.870	-0.750	1		

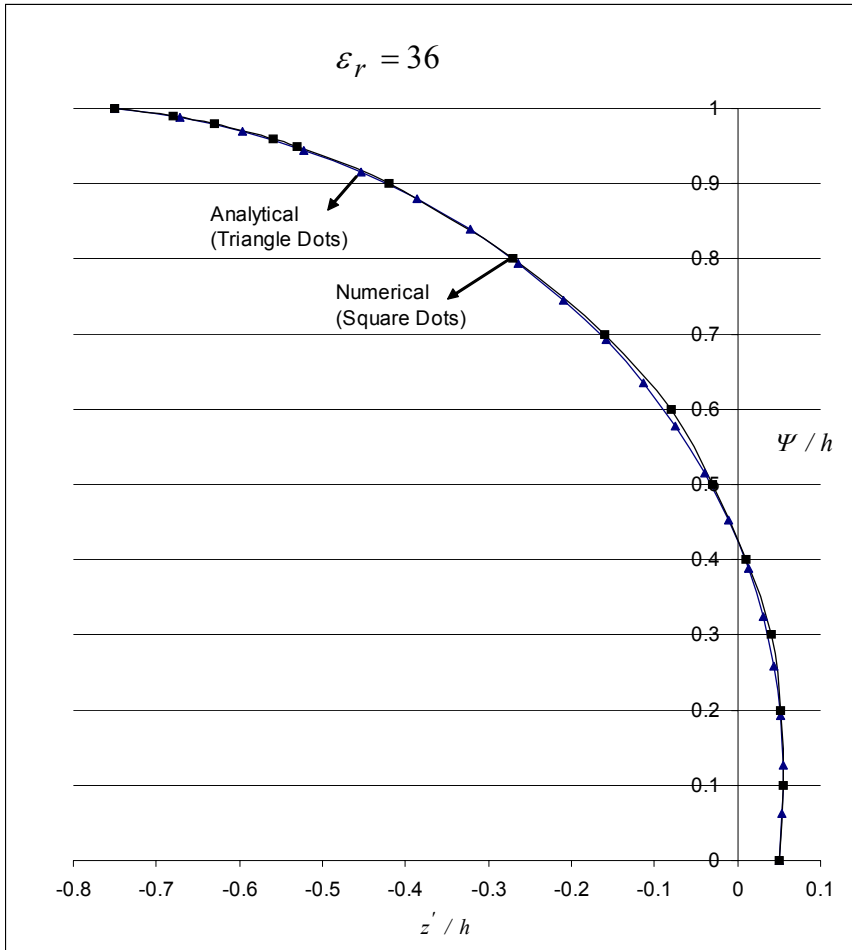


Figure 6. Lens Boundary Curve Numerical Solution for $\varepsilon_r = 36$

Table 3. θ_{1max} , θ_{2max} , z'/h and Ψ/h Values for $\varepsilon_r = 36$

Analytical		Numerical	
θ_1 °	θ_2 °	z'/h	Ψ/h
0	0	0.05	0
4.5	50.055	0.053	0.063
9	66.752	0.055	0.127
13.5	74.854	0.052	0.193
18	80.232	0.044	0.258
22.5	84.445	0.031	0.324
27	88.062	0.013	0.389
31.5	91.338	-0.011	0.453
36	94.404	-0.040	0.516
40.5	97.333	-0.074	0.577
45	100.169	-0.114	0.636
49.5	102.941	-0.159	0.692
54	105.668	-0.209	0.745
58.5	108.363	-0.264	0.794
63	111.035	-0.323	0.839
67.5	113.691	-0.386	0.879
72	116.336	-0.453	0.915
76.5	118.974	-0.523	0.945
81	121.608	-0.596	0.969
85.5	124.239	-0.672	0.988
90	126.87	-0.75	1

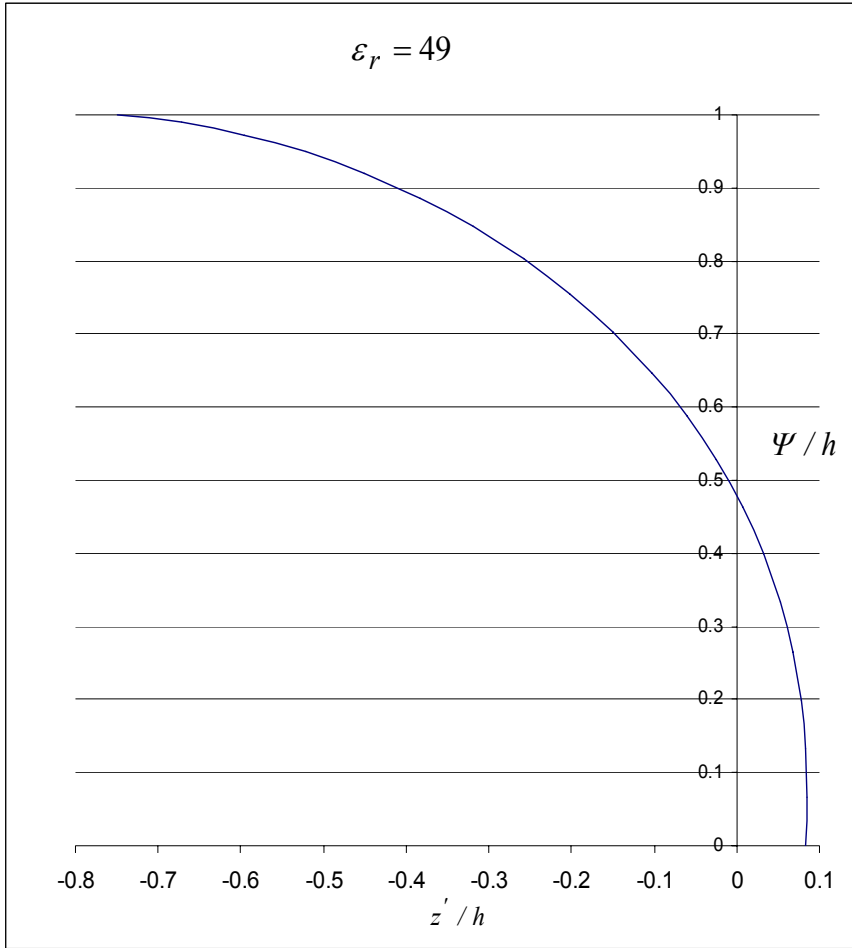


Figure 7. Lens Boundary Curve Analytical Solution for $\varepsilon_r = 49$.

Table 4. θ_{1max} , θ_{2max} , z' / h and Ψ / h Values for $\varepsilon_r = 49$.

θ_1°	θ_2°	z' / h	Ψ / h
0	0	0.0833	0
4.5	37.977	0.084	0.066
9	57.731	0.083	0.132
13.5	68.478	0.078	0.199
18	75.549	0.069	0.266
22.5	84.130	0.053	0.333
27	85.293	0.033	0.399
31.5	89.150	0.007	0.464
36	92.657	-0.024	0.527
40.5	95.931	-0.061	0.588
45	99.043	-0.103	0.647
49.5	102.040	-0.150	0.703
54	104.951	-0.202	0.755
58.5	107.799	-0.258	0.803
63	110.599	-0.318	0.847
67.5	113.363	-0.383	0.886
72	116.099	-0.451	0.920
76.5	118.813	-0.522	0.949
81	121.510	-0.596	0.972
85.5	124.195	-0.672	0.989
90	126.870	-0.75	1

4. Increase in Electric Field due to Passage Through Dielectric Boundary

We will have an increase in electric field due to propagation from the dielectric lens to air. This increase can be found by the transmission coefficient as(for rays normally incident to the lens boundary)

$$T = \frac{2}{1 + 1/\sqrt{\epsilon_r}} \quad (4.1)$$

The increases in electric field for different ϵ_r values are presented in table 5.

Table 5. Transmission Coefficients for different ϵ_r values

ϵ_r	25	36	49
T	1.67	1.71	1.75

5. Dielectric Breakdown

One of the most important design parameters for launching lens design is dielectric breakdown and insulation. In general, to eliminate the dielectric breakdown problem and for insulation purposes oil which has a dielectric constant of $\epsilon_r = 2.26$ is used as a container for launching lenses. However, in our case we should have at least $\epsilon_r = 25$ for this special kind of launching lens. Therefore, our lens dielectric constant should be

$$\epsilon_{r\text{lens}} = 2.26 * 25 = 56.5 \quad (5.1)$$

Figure 10 presents the spherical lens, launching lens and IRA geometry.

While designing the feeding of an IRA, one should avoid to use the dielectric material that has high ϵ_r because of dispersion and loss. Therefore, instead of using oil for the spherical lens we may use SF₆ (Sulfur hexafluoride) which has an approximate dielectric constant of $\epsilon_r = 1$. SF₆ is a gas that is commonly used for HPEM applications. It has a breakdown strength almost triple that of air at one atmosphere, increasing for higher pressure. However, for mechanical reasons, one may want to limit the pressure. For a few 100 kV, one can thereby keep the lens radius to no-too-many cm.

Detailed calculations on the switch geometry and how it interfaces with the lens should be done to minimize the risetime.

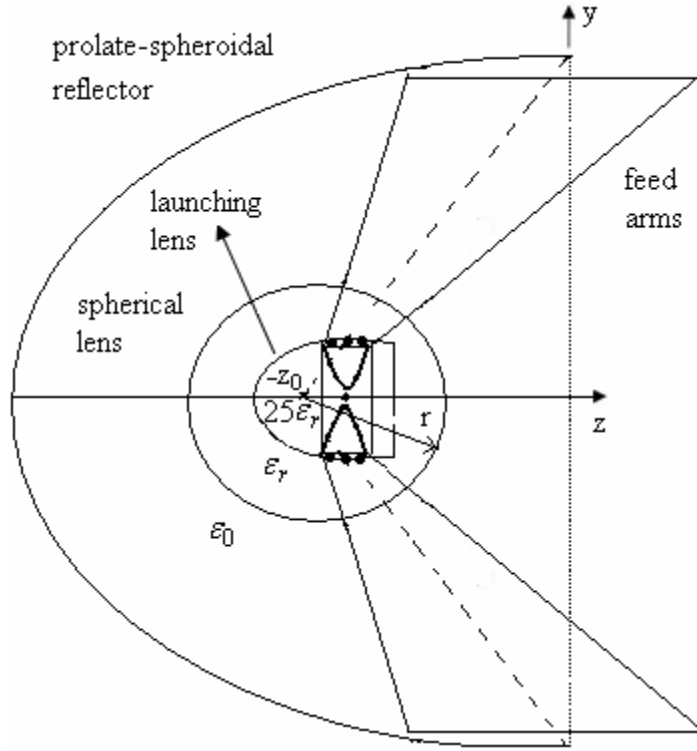


Figure 10. Spherical Lens, Launching Lens and IRA Geometry

6. Prepulse Dispersion

As discussed in early papers [4], the prepulse term subtracts from the impulse at the second focal point of a Prolate-Spheroidal IRA. By adding an additional part as shown in figure 11, we will have dispersion in the prepulse and this will give us an increase in the impulse.

One can see a geometry that is suggested for dispersion in the prepulse. This part of the lens should be made from oil or polyethylene which has a dielectric constant of $\epsilon_r = 2.26$.

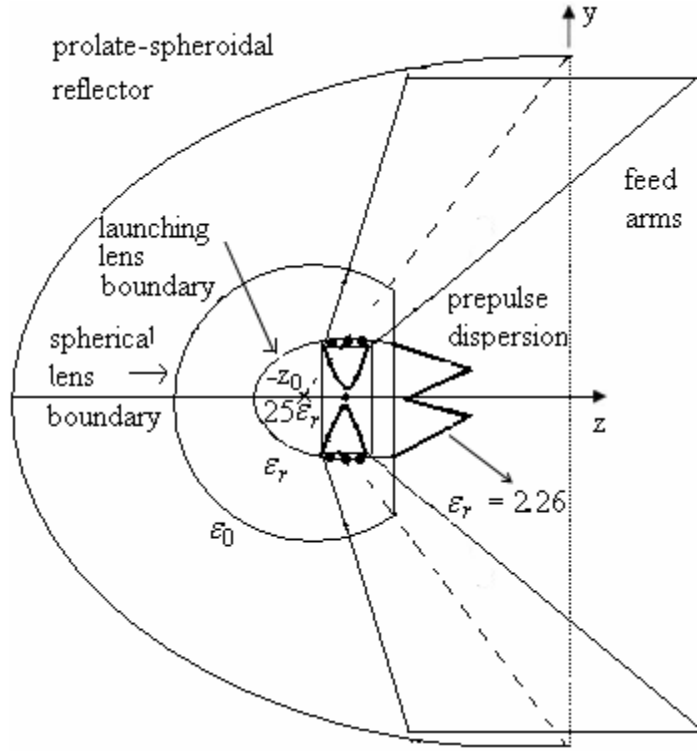


Figure 11. Addition of a Part for Dispersion in the Prepulse(oil or polyethylene)

7. Determining h

Determining the dimensions of the lens or the geometric parameter h is an experimental and numerical problem. The bigger h gives less dielectric breakdown. However, we have to deal with loss and dispersion as a price for bigger h values.

8. Conclusion

We are designing a lens such that within the lens we have a spherical TEM wave centered on the switch center. However, outside the lens we have an approximate spherical TEM wave which is centered at the first focal point of the prolate-spheroidal IRA. Diverging a spherical TEM wave to another diverging spherical TEM wave is the key point of this design. Different dielectric constants give different lens geometries. We have designed three different lenses for $\epsilon_r = 25, 36$ and 49 .

One of the most important contributions of this paper is designing a launching lens for a prolate-spheroidal IRA that has a $\theta_{2\max} > 90^\circ$. Therefore we consider both \pm roots in (2.7). Because of the dielectric breakdown, we have suggested the use of an additional spherical lens as a container. Finally, a different geometry is proposed to obtain less prepulse amplitudes at the focal point. We also discussed the determination of the height of the launching lens h briefly.

References

1. C. E. Baum , J. J. Sadler and A. P. Stone “A Uniform Dielectric Lens for Launching a Spherical Wave into a Paraboidal Reflector”, SSN 360, July 1993.
2. D.V. Giri et al., 1997, “Design, fabrication, and testing of a paraboidal reflector antenna and pulser system for impulse-like waveforms,” IEEE Trans. Plasma Science, vol. 25, pp. 318-326, April.
3. D.V. Giri at all. “A reflector antenna for radiating impulse-like waveforms”, SSN 382, July 1995.
4. S. Altunc, C. E. Baum, C. Christodoulou, E. Shamiloglu, and G. Buchenaur, “Focal waveforms for various source waveforms driving a prolate-spheroidal impulse radiating antenna,” Radio Sci., Feb. 2008, RS003775.